




Random uptake of nanoparticles by cells and negative binomial distributions of pits

Vladimir Sholokhov^{1,a}, Dmitri V. Alexandrov^{1,b}, Eugeniya V. Makoveeva^{1,c}, Margarita A. Nikishina^{1,d}, Vladimir Y. Shur², Ekaterina V. Shishkina², Marina P. Sutunkova³, Ilzira A. Minigalieva³, Yulia V. Ryabova³, Larisa I. Privalova³, and Sergei Fedotov^{4,e} 

¹ Laboratory of Stochastic Transport of Nanoparticles in Living Systems, Laboratory of Multi-Scale Mathematical Modeling, Department of Theoretical and Mathematical Physics, Ural Federal University, Lenin Ave., 51, Ekaterinburg 620000, Russian Federation

² School of Natural Sciences and Mathematics, Ural Federal University, Lenin ave., 51, Ekaterinburg 620000, Russian Federation

³ Yekaterinburg Medical Research Center for Prophylaxis and Health Protection in Industrial Workers, 30 Popov Street, Yekaterinburg 620014, Russian Federation

⁴ Department of Mathematics, The University of Manchester, Manchester M13 9PL, UK

Received 11 April 2024 / Accepted 19 June 2024

© The Author(s) 2024

Abstract This paper focuses on a key experimental observation concerning the random internalization of nanoparticles by cells: the occurrence of over-dispersion in nanoparticle uptake which can be characterized by a negative binomial distribution. We compare the well-known distribution with the empirical distribution of pits on the surface of an alveolar macrophage. We find that a negative binomial distribution provides the accurate curve-fit model for the observed pit distribution.

1 Introduction

Uncovering the mechanisms of how cells uptake nanoparticles is essential for ensuring the safe and efficient application of these particles in medicine [1–5]. Many experiments have been conducted to study the uptake of nanoparticles [6, 7]. It has been found that cellular uptake is influenced by a range of factors such as size and shape of nanoparticles, membrane characteristics, experimental conditions, etc. [8–13]. Even though the interaction of a single nanoparticle with cells exhibits microscale randomness, predictability across entire populations can be upheld by describing it with conventional statistical distributions [14]. The stochastic generation nanoparticle-loaded vesicles (NLVs) could be expected to follow Poisson distribution. However, Summers et al. [14] found that a variance exceeded the mean. It prompts them to adopt an over-dispersed probability distribution model. This model accounts for Poisson processes with multiple rate constants and describes the observed data across various nanoparticle loading scenarios. Rees et al. [15] performed experiments focused on the internalization of 8nm quantum dot nanoparticles through endocytosis in human alveolar epithelial cells (A549) and human bronchial epithelial cells (BEAS-2B). These cells were exposed to various combinations of nanoparticle dosage and exposure duration. Their findings revealed that the probability distribution for the NLVs per cell exhibits over-dispersion. Rees et al. found that a negative binomial distribution is the best curve-fit model of the measured NLVs distribution. They suggested a probabilistic model in which the generation of endosomes on the cell membrane can be described by a spatiotemporal Poisson process that is dependent of the area of the cells. They assumed that the cell area across a population is gamma-distributed and this leads to the *negative binomial distribution* for nanoparticle-loaded vesicles.

^a e-mail: vladimir.sholokhov@urfu.ru

^b e-mail: dmitri.alexandrov@urfu.ru

^c e-mail: e.v.makoveeva@urfu.ru

^d e-mail: margarita.a.nikishina@gmail.com

^e e-mail: sergei.fedotov@manchester.ac.uk (corresponding author)

Katsnelson et al. [16, 17] and Privalova et al. [18] conducted a series of experiments examining the phagocytic activity of the rat's pulmonary macrophages and neutrophil leukocytes. Intratracheal instillation of a water suspension containing nanoparticles was used to examine the response of the lower airways to nanoparticles. The authors analyzed the ultrastructural damage to the cell surface caused by the nanoparticles and their intracellular localization. The topology of the cell surfaces of macrophages was examined using semi-contact atomic force microscopy. Multiple pits are observed on the surfaces of alveolar macrophages. The size of these pits increases with the size of nanoparticles. Additionally, smaller nanoparticles result in a higher surface concentration of pits. These pits are believed to be a result of the initial stage of active endocytosis rather than mere "footprints" left by particles passively penetrating the cell membrane and creating a hole. Also, note that the clustering of particles on the cell membrane during the uptake process was studied in Ref. [19]. In addition, nanoparticle clustering in the steady-state and unsteady conditions using the Smoluchowski coagulation equation for the fusion of endosomes was analytically studied in Refs. [20–22].

The main aim of this paper is to compare the well-known distribution and those of multiple pit on the surfaces of an alveolar macrophage [16–18]. Our intention is to show that a negative binomial distribution provides an accurate curve-fit model for the experimentally observed pit distribution on a single cell.

2 Distribution of pits on the surface of the alveolar macrophage

The aim of this section is to compare the theoretical distribution, such as the negative binomial distribution [23]

$$p(k) = \frac{\Gamma(a+k)}{k! \Gamma(a)} (1-p)^k p^a, \quad k = 0, 1, 2, \dots \quad (1)$$

with the empirical distribution of pits on the surface of a single alveolar macrophage. Here p is the probability lying within the interval $[0, 1]$ and a is a positive parameter. Katsnelson et al. [16, 17], Privalova et al. [18] analysed the phagocytic activity of pulmonary macrophages obtained from rats that are given intratracheal instillation of a water suspension containing silver, gold, iron oxide, and copper oxide nanoparticles. Control experiments are also conducted using deionized water without any nanoparticles. The topology of cell surfaces of pulmonary macrophages was analyzed by semi-contact atomic force microscopy. In Fig. 1, numerous pits are clearly visible on the surface of alveolar macrophages (picture below) in stark contrast to the nearly smooth surface of cells

Fig. 1 Alveolar macrophage surface topography visualized by the semi-contact atomic force microscopy: control (pictured above) and after instillation of a suspension containing copper oxide nanoparticles with an average diameter of 20 nm (scan size $2 \times 2 \mu\text{m}$). The average pit diameter 25.2 ± 0.9 nm corresponds to the mean diameter of nanoparticles (see details in [18])

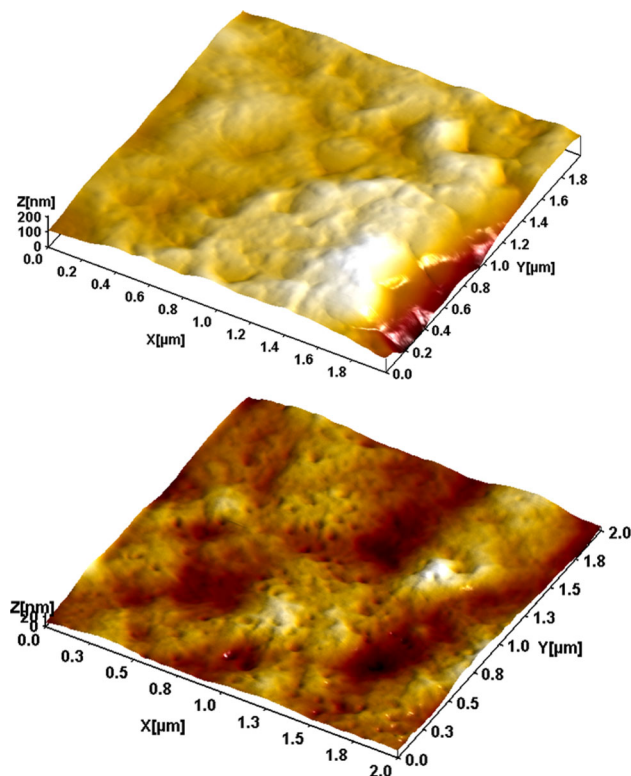


Fig. 2 The surface topography of a rat alveolar macrophage (scan size 500×500 nm) after the intratracheal instillation of a suspension containing copper oxide nanoparticles with an average diameter of 20 nm. Semi-contact atomic force microscopy was employed to examine the surface topology

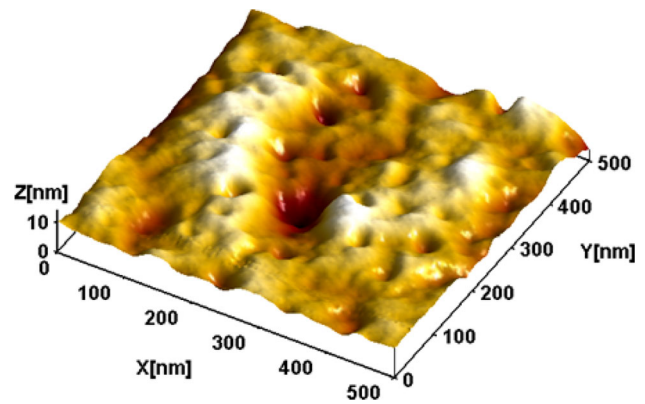
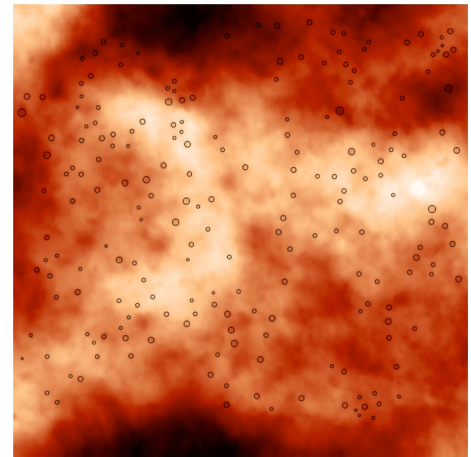


Fig. 3 Processed image of the macrophage surface of 4 square microns involving copper oxide nanoparticles with an average diameter of 20 nm. Pits on the surface of an alveolar macrophage are encircled for better visualization [16–18, 24]



from control rats (pictured above). The surface pits observed are a consequence of plasma membrane invagination during the phagocytosis of copper oxide nanoparticles with an average diameter of 20 nm (scan size $2 \times 2 \mu\text{m}$).

Figure 2 displays a smaller scan size (500×500 nm) that provides finer details and improves the visualization of pits on the surface of a rat alveolar macrophage. Figure 3 shows a processed image of the macrophage surface involving copper oxide nanoparticles with an average diameter of 20 nm. Micro-pits are encircled for better visualization. It was suggested that these pits were the result of the invagination of the plasma membrane during the phagocytosis of copper oxide nanoparticles. We think that the obtained data are universal and suitable for other metal-containing nanoparticles.

One of the purposes of this paper is to obtain the empirical distribution of pits on the surface of a pulmonary macrophage. We divide the macrophage’s area into N small areas S_0 and count the number of areas, N_k , with exactly k pits. The normalized empirical distribution can be obtained as N_k/N (see Fig. 4). We also count the number of pits x_i on the i th small area, the total number of pits $n = \sum_k kN_k$ and find the corresponding average density $\lambda_0 = n/(NS_0)$ per unit area. SIAMS Photolab 4 was used for pit identification. We estimate empirical *mean* and *var* as follows:

$$\text{mean} = \frac{1}{N} \sum_{i=1}^N x_i, \quad \text{var} = \frac{1}{N-1} \sum_{i=1}^N (x_i - \text{mean})^2. \quad (2)$$

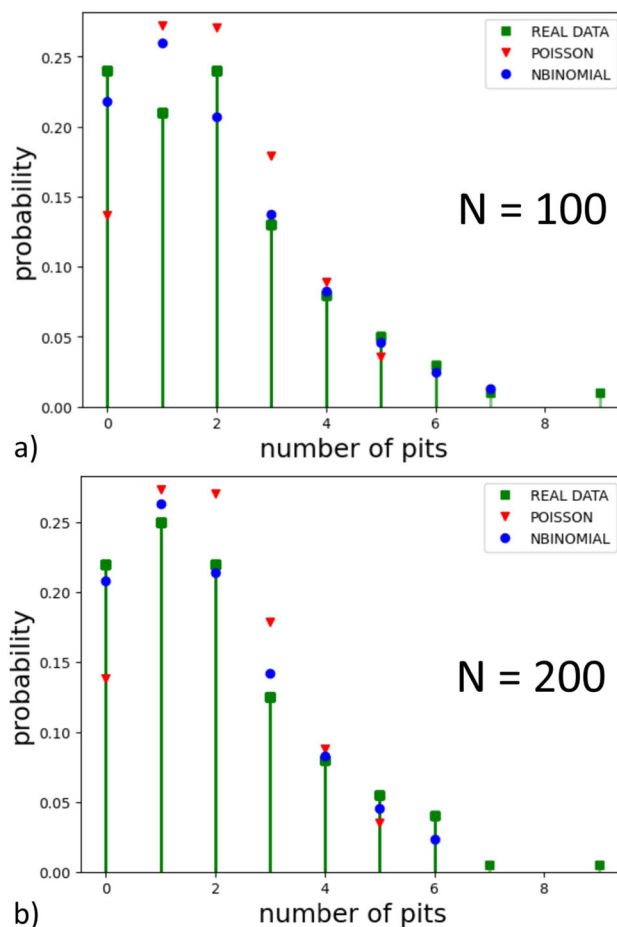
Figure 4 illustrates the empirical distribution (in green), Poisson distribution (represented by red triangles), and negative binomial distribution (depicted as blue circles) for the number of pits on the cell’s surface with an area of $S_0 = 0.04 \mu\text{m}^2$. Two different sample sizes are presented: (a) $N = 100$ and (b) $N = 200$. In both cases of sampling, we observe a noticeable overdispersion. For case (a) with $N = 100$, the empirical mean is 1.99, and the variance is 3.32. For case (b) with $N = 200$, the empirical mean is 1.98 and the variance is 3.10. Since the well-known Poisson distribution

$$P(k) = \frac{(\lambda S_0)^k e^{-\lambda S_0}}{k!} \quad (3)$$

Fig. 4 a $N = 100$.

Empirical (green), Poisson (red triangles), and negative binomial distributions (blue circles) for the number of pits on the cell's surface with area $S_0 = 0.04 \mu\text{m}^2$. Empirical mean and variance are 1.99 and 3.32. For the negative binomial distribution, the log-likelihood value is -185.1 , and for the Poisson distribution, it is -192.42 . Parameters $a = 2.97$ and $p = 0.59$ in (1) are obtained by maximum likelihood estimation.

b $N = 200$. Empirical mean and variance are 1.98 and 3.10. For the negative binomial distribution with $a = 3.51$ and $p = 0.63$, the log-likelihood value is -366.91 , and for the Poisson distribution, it is -378.26



has a mean equal to its variance, it does not fit our data well. Here S_0 is the cell surface and λ is the rate of Poisson distribution per unit area per unit time. It is clear from Fig. 4 that the negative binomial distribution (blue circles) for $N = 200$ provides a strong fit for the empirical distribution. It is also evident from Fig. 4 that an increase in the sample size leads to a more accurate fitting of the negative binomial distribution to the empirical data, particularly for smaller values of the number of pits, such as $k = 0, 1, 2$. Clearly, the Poisson distribution (red triangles) is a poor fit for our data.

To select the more suitable fit for the empirical distribution N_k quantitatively, we compare the likelihood values of the negative binomial distribution (1) and the Poisson distribution (3). We employ maximum likelihood estimation to get the parameters of two models. Note that the log-likelihood function represents the natural logarithm of the likelihood function \mathcal{L} , which is the probability density of experimental points x treated as a function of the parameters of a statistical model, i.e. $\mathcal{L}(\theta|x) = p_\theta(x) = P_\theta(X = x)$, where θ is the actual parameter, X is a discrete random variable, p is the probability mass function and P is the posterior probability of θ given the data x . We found that the negative binomial distribution has a higher log-likelihood value in both cases. For $N = 100$, the log-likelihood value for the negative binomial distribution is -185.1 , whereas for the Poisson distribution, it is -192.42 . For the case $N = 200$, the negative binomial distribution has also a higher log-likelihood value, -366.91 , compared to the Poisson distribution, -378.26 . Therefore, based on likelihood values, the negative binomial distribution provides a better fit for our dataset. Since the empirical distribution N_k/N has a heavier tail than the Poisson distribution (see Fig. 4), it indicates the heterogeneity of nanoparticle uptake.

3 Conclusions

In summary, we represent and analysed the experimental data on nanoparticles uptake by a rat alveolar macrophage. We revealed that the pits on the macrophage surface are caused by the invagination of plasma membrane during the phagocytosis of copper oxide nanoparticles. In this paper, we have carried out the statistical analysis of pit distribution on the surface of a single macrophage relies on a limited sample of 100 and 200

sub-regions. Taking this into account, we demonstrate that the negative binomial distribution, in contrast to the Poisson distribution, provides a more accurate model for experimentally observed pits on a single cell surface. Also, with increasing sampling, the negative binomial distribution delivers a strong fit for the empirical distribution. We also confirm that the nanoparticles are absorbed heterogeneously by the cell. Comprehensive statistical analysis of the pit distribution on the surfaces of pulmonary macrophages and neutrophil leukocytes and a number of nanoparticles inside cells will be provided in future publications. However, we should note that the distribution (1) for nanoparticle-loaded vesicles has already been experimentally validated by Rees et al. [15] and, therefore, allows us to believe that nanoparticles random uptake obeys the negative binomial distribution of pits on the cell surface.

Acknowledgements V.D.S., D.V.A., E.V.M., M.A.N., I.A.M. and Y.V.R. gratefully acknowledge the research funding from the Ministry of Science and High Education of the Russian Federation (Ural Federal University Program of Development within the Priority-2030 Program). The equipment of the Ural Center for Shared Use “Modern nanotechnology” Ural Federal University (Reg no. 2968), which is supported by the Ministry of Science and Higher Education RF (Project no. 075-15-2021-677) was used.

Funding Ministry of Science and High Education of the Russian Federation (Priority-2030 Program, 075-15-2021-677).

Data availability No data associated with the manuscript.

Open Access This article is licensed under a Creative Commons Attribution 4.0 International License, which permits use, sharing, adaptation, distribution and reproduction in any medium or format, as long as you give appropriate credit to the original author(s) and the source, provide a link to the Creative Commons licence, and indicate if changes were made. The images or other third party material in this article are included in the article’s Creative Commons licence, unless indicated otherwise in a credit line to the material. If material is not included in the article’s Creative Commons licence and your intended use is not permitted by statutory regulation or exceeds the permitted use, you will need to obtain permission directly from the copyright holder. To view a copy of this licence, visit <http://creativecommons.org/licenses/by/4.0/>.

References

1. H. Hillaireau, P. Couvreur, *Cell. Mol. Life Sci.* **66**, 2873 (2009)
2. T.G. Iversen, T. Skotland, K. Sandvig, *Nano Today* **6**(2), 176 (2011)
3. N.D. Donahue, H. Acar, S. Wilhelm, *Adv. Drug Deliv. Rev.* **143**, 68 (2019)
4. R. Augustine, A. Hasan, R. Primavera, R.J. Wilson, A. Thakot, B.D. Kevadiya, *Mater. Today Commun.* **25**, 101692 (2020)
5. M.S. de Almeida, E. Susnik, B. Drasler, P. Taladriz-Blanco, A. Petri-Fink, B. Rothen-Rutishauser, *Chem. Soc. Rev.* **50**(9), 5397 (2021)
6. H.J. Shin, M. Kwak, S. Joo, J.Y. Lee, *Sci. Rep.* **12**(1), 20146 (2022)
7. Y. Boinapalli, R.S. Pandey, A.S. Chauhan, M.S. Sudheesh, *Int. J. Pharmac.* **632**, 122579 (2023)
8. A. Lesniak, A. Salvati, M.J. Santos-Martinez, M.W. Dawson, C. Aberg, *J. Amer. Chem. Soc.* **135**, 1438 (2013)
9. K. Kettler, K. Veltman, D. van De Meent, A. van Wezel, A.J. Hendriks, *Env. Toxic. Chem.* **33**(3), 481 (2014)
10. S. Dasgupta, T. Auth, G. Gompper, *Nano Lett.* **14**(2), 687 (2014)
11. C. Aberg, V. Piattelli, D. Montizaan, A. Salvati, *Nanoscale* **13**(41), 17530 (2021)
12. X. Yi, H. Gao, *Nanoscale* **9**(1), 454 (2017)
13. X. Liu, T. Auth, N. Hazra, M.F. Ebbesen, J. Brewer, G. Gompper, J.J. Crassous, E. Sparr, *Proc. Nat. Acad. Sci.* **120**(30), e2217534120 (2023)
14. H.D. Summers, P. Rees, M.D. Holton, M. Rowan Brown, S.C. Chappell, P.J. Smith, R.J. Errington, *Nat. Nanotech.* **6**(3), 170 (2011)
15. P. Rees, J.W. Wills, M.R. Brown, C.M. Barnes, H.D. Summers, *Nat. Commun.* **10**(1), 2341 (2019)
16. B.A. Katsnelson, L.I. Privalova, M.P. Sutunkova, M.Y. Khodos, V.Y. Shur, E.V. Shishkina, L.G. Tulakina, S.V. Pichugova, J.B. Beikin, *J. Nanomed. Nanotech.* **3**, 1 (2012)
17. B.A. Katsnelson, L.I. Privalova, M.P. Sutunkova, V.B. Gurvich, N.V. Loginova, I.A. Minigalieva, E.P. Kireyeva, V.Y. Shur, E.V. Shishkina, Y.B. Beikin, O.H. Makeyev, I.E. Valamina, *Int. J. Nanomed.* **10**, 3013 (2015)
18. L.I. Privalova, B.A. Katsnelson, N.V. Loginova, V.B. Gurvich, V.Y. Shur, Y.B. Beikin, M.P. Sutunkova, I.A. Minigalieva, E.V. Shishkina, S.V. Pichugova, L.G. Tulakina, S.V. Beljayeveva, *Int. J. Mol. Sci.* **15**(11), 21538 (2014)
19. H. Jin, D.A. Heller, R. Sharma, M.S. Strano, *ACS Nano* **3**, 149 (2009)
20. D.V. Alexandrov, N. Korabel, F. Currell, S. Fedotov, *Cancer Nanotechnol.* **13**, 15 (2022)
21. E.V. Makoveeva, D.V. Alexandrov, S.P. Fedotov, *Crystals* **12**, 1159 (2022)
22. E.V. Makoveeva, *Math. Meth. Appl. Sci.* **47**, 6746 (2024)
23. W. Feller, *An Introduction to Probability Theory and Its Applications* (Wiley, NY, 1968)

24. B. Katsnelson, L.I. Privalova, S.V. Kuzmin, T.D. Degtyareva, M.P. Sutunkova, O.S. Yermenko, I.A. Minigalieva, E.P. Kireyeva, M.Y. Khodos, A.N. Kozitsina, N.A. Malakhova, J.A. Glazyrina, V.Y. Shur, E.I. Shishkin, E.V. Nikolaeva, *Int. J. Occup. Env. Health* **16**(4), 508 (2010)